Energy and Buildings 87 (2015) 199–210

Contents lists available at ScienceDirect

Energy and Buildings

journal homepage: www.elsevier.com/locate/enbuild

Model predictive control of radiant slab systems with evaporative cooling sources

Jingjuan (Dove) Feng[a,*], Frank Chuang[b], Francesco Borrelli[b], Fred Bauman[c]

[a] Department of Architecture, University of California, Berkeley, USA
[b] Department of Mechanical Engineering, University of California, Berkeley, USA
[c] Center for the Built Environment, University of California, Berkeley, USA

ARTICLE INFO

Article history:
Received 5 June 2014
Received in revised form
10 November 2014
Accepted 13 November 2014
Available online 24 November 2014

Keywords:
Radiant slab systems
Evaporative cooling
Model predictive control
Energy and comfort performance
Calibrated simulation

ABSTRACT

Buildings that use radiant slab systems with evaporative cooling sources have shown to be energy efficient. However, control of the systems is challenging because of the slow response of the slab and the limited capacity of cooling sources. The objectives of this paper are to: (1) create a simplified dynamic model of radiant slab system for implementation in real-time model predictive controller (MPC); and (2) test the MPC energy and thermal comfort performance in a case study building. A calibrated EnergyPlus model of the building was developed as the testbed. The MPC is compared with the existing rule-based control method for a cooling season in a dry and hot climate. The results indicated that the MPC controller was able to maintain zone operative temperatures at EN 15251 Category II level more than 95% of the occupied hours for all zones, while with the rule-based method, only the core zone were maintained at this thermal comfort level. Compared to the rule-based method, MPC reduced the cooling tower energy consumption by 55% and pumping power consumption by 25%.

1. Introduction

Interest and growth in radiant slab cooling and heating systems have increased in recent years because they have been shown to be energy efficient in comparison to all-air distribution systems [1,2]. Radiant slab systems circulate cooling/heating water through the adjacent building structure and deliver more than 50% of the total sensible heat flux for building space conditioning by thermal radiation [3]. Utilizing large surfaces for heat exchange, the temperature of the cooling/heating water can be only a few degrees lower/higher than the room air temperature. This small temperature difference allows improvement on plant side equipment efficiency, or the use of alternative cooling/heating sources such as solar, evaporative processes, and ground heat exchange. There is a large body of literature that have studied the principles of designing radiant slab cooling systems including cooling load calculation methods [4,5], the use of operative temperature for comfort control [6], and the estimation of cooling capacity [7,8]. However, optimal control and operation of the systems remains a challenge, and the potential energy and thermal comfort benefits would not be achieved without operational practices that can accompany the strengths of the radiant systems [2].

Compared to air systems, radiant systems present many challenges in terms of control. With water pipes embedded in radiant layers, hydronic radiant systems are slow to respond to control signals due to large thermal inertia. The response time depends on the depth of the tubing and the heat capacity of the radiant slab. Usually the time constant can be up to a couple hours [3]. Because of this, sudden load changes in the thermal space cannot be compensated for by the control system. Conventional control methods, such as PI control, may not be able to maintain thermal comfort and can lead to high energy consumption caused by constant switchover between heating and cooling mode in an effort to maintain a constant room temperature [2]. Another key potential energy benefits of radiant slab systems is their capability to shift load to unoccupied hours. Load shifting consists of shaping the energy profile delivered to a building, and thereby exploiting the possibility of storing energy for later use. Thermal storage is inherent to a building's structure and radiant slab systems are built to enhance this feature [9]. Previous researches indicated that optimal profile of delivered energy depends on various factors which include time varying utility prices, availability of renewable energy, and internal (people/lighting) and external (solar/ambient temperature)

* Corresponding author at: 1080 Marina Village Pkwy, Alameda, CA 94501, USA. Tel.: +1 5103663139.
E-mail address: dovefeng@gmail.com (J. Feng).

http://dx.doi.org/10.1016/j.enbuild.2014.11.037
0378-7788/

Nomenclature

T_a	air temperature in the room, °C
T_s	radiant surface temperature, °C
m_a	mass of air in room, kg
C_p	specific heat capacity of air, J/kg K
$\dot{m}_{a_{in}}$	mass flow rate of air into the room, kg/s
$T_{a_{in}}$	temperature of air flowing into room, °C
P_{in}	heat generated by elements inside the room, W
P_{dis}	disturbance flow, W
α	fraction of solar radiation absorbed by slab
β	fraction of internal heat/radiation absorbed by slab
G_s	radiation generated in or incident on the room, W
U_{rs}	heat transfer coefficient between room and slab, W/m^2 K
A_{rs}	surface area in contact between room and slab, m^2
$T_{z,i}$	temperature of adjacent zone i, °C
$U_{ra,i}$	heat transfer coefficient between room and zone i, W/m^2 K
$A_{ra,i}$	surface area in contact between room and zone i, m^2
T_{w_o}	temperature of water at exit of water pipe, °C
T_{w_i}	temperature of water at inlet of water pipe, °C
$\dot{m}_{w_{in}}$	mass flow rate of water into the slab, kg/s
D	diameter of water pipe in slab, m
L	total length of water pipe in slab, m
U_w	heat transfer coefficient between water and slab, W/m^2 K
$C_{p,w}$	specific heat capacity of water, J/kg K
q_w	heat exchange between water and slab, W
m_s	mass of slab, kg
$C_{p,s}$	specific heat capacity of slab, J/kg K

load variation [10–12]. This is a very complex problem and is challenging for the traditional heuristic rule based control methods to tackle it successfully.

In the literature, some early reports on rule based control methods for radiant slab systems include Olesen [13,14], Antonopoulos [15] and Weitzmann [16], the latter gave a short overview of the proposed control-concepts. Some common properties of the algorithms include: (a) adjustment of water supply temperature set point is a function of outside air temperature; (b) self-regulation of the concrete slab conditioning system is assumed to be sufficient; and (c) heating and cooling operation are enabled or activated depending on the season and/or outside air temperature. These rule-based control models have been mostly derived empirically from simulations or steady-state physical models so it is hard to expand their applicability.

A more advanced control method was developed by Gwerder et al. [17–19], who proposed a pulse-width modulated (PMV) intermittent operation of water circulation pump, combined with supply water temperature control. Their method aimed to take into account uncertainties in load disturbance when achieving both comfort criteria and energy efficiency. However, there is no documentation on the application or validation of their method.

More recently, model predictive control (MPC) has become popular in the building industry [20–22]. MPC is a flexible and well-developed advanced control technique with broad applications in complex systems. Its optimization and prediction features make it particularly advantageous in the application of radiant slab systems. Gayeski [23] presented a study focused on optimizing the control of a low-lift chiller serving a radiant slab system. The energy consumption of the cooling system, including chiller, compressor, condenser fan and chilled water pump, was minimized. They modeled the thermal responses of a test chamber using the inverse transfer function model [24], where room temperatures can be predicted based on thermal load conditions. Corbin et al. [25] developed an MPC environment integrating Matlab and EnergyPlus to predict optimal building control strategies. The environment was used to determine hourly supply water temperature and pump operation availability that minimize daily energy consumption for a small office building that uses a radiant slab system. One common feature of MPC control is high computational requirements due to model complexity and the optimization process. This is perceived by practitioners as a major obstacle in terms of the applicability and scalability. To reduce the computational intensity during real time operation, Coffey [26] proposed a method to use look-up tables that is pre-generated with a MPC to obtain near optimum control decisions. He demonstrated its application to the control of an abstract single zone radiant cooling system modeled in EnergyPlus. For the same purpose, Ostendorp et al. [27] investigated the method of extracting supervisory rules from the MPC generated optimum control strategies. They tested the method for controlling the radiant slab and ventilation system in a test cell, and showed that the rules were capable of reproducing nearly all of the energy and comfort benefits of the MPC solutions for the tested cases.

In summary, MPC is a promising technique for the realization of the energy benefits of radiant slab systems. The objectives of this paper are to: (1) create a simplified dynamic model of radiant slab system for easy implementation in real-time model predictive controller; and (2) implement the MPC in a case study building to demonstrate its application and test its performance. An calibrated EnergyPlus model of the building was developed as the testbed. The MPC is compared with the existing rule-based control method for both energy and thermal comfort performance.

2. Methodology

To assess the efficacy of various control techniques for radiant slab systems, we must create a flexible testbed with which to implement the controllers. We choose to create a calibrated EnergyPlus model of a test building conditioned by radiant system. EnergyPlus was selected because it employs the fundamental heat balance method for zone thermal modeling and has been validated against experimental measurements and through comparative testing with BESTest suite [28–30]. In addition, it is one of the limited number of tools that is capable of accurately simulating radiant system performance [5,31]. The procedure for our work is outlined below:

- Create and calibrate EnergyPlus model of the case study building and its associated HVAC system.
- Derive simplified dynamic models from the EnergyPlus model for MPC controller design.
- Design MPC controller for the radiant system.
- Implement and test a fine-tuned rule-based control strategy and the MPC controller on the EnergyPlus model.
- Create and compare metrics for thermal comfort and energy consumption of the controllers.

There are two main advantages of using an EnergyPlus model of a real building versus a fictitious building for the test: (1) the radiant slab model in EnergyPlus can be validated against field measurement data; (2) the utility bill and monitored long-term data from a real building can be used to improve the predictability of EnergyPlus model for energy and thermal comfort performance.

3. The case study building: David Brower Center (DBC)

The David Brower Center (DBC) is a 4-story 4042 m^2 office building located in downtown Berkeley, California, which is at

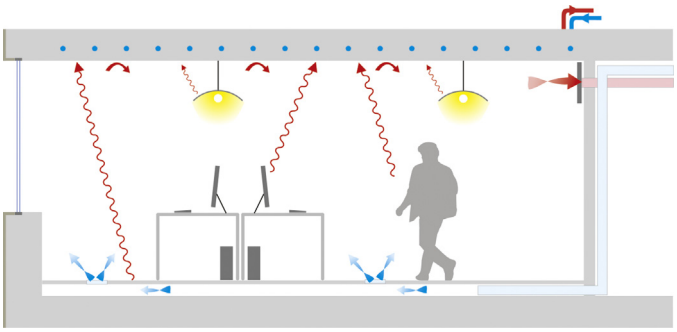

Fig. 1. Radiant slab with under floor air distribution (UFAD) system.

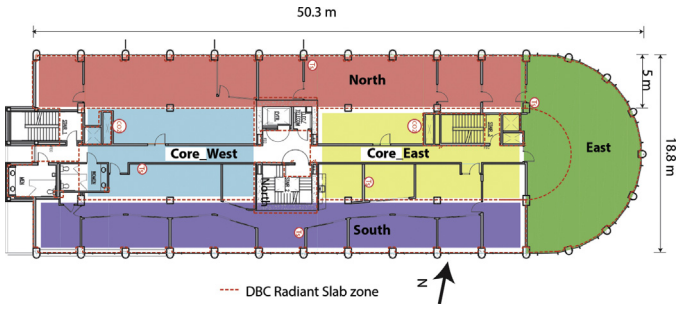

Fig. 2. Typical floor plan of DBC building and radiant system zoning.

about 37.8 °C north latitude with a climate classified as mild with moderate temperatures year around. The 0.4% cooling design temperatures (dry bulb/wet bulb) are 27.7 °C and 18.3 °C, and the 99.6% heating design temperature is 2.9 °C. The building was completed and first occupied in 2009. It contains a lobby and public meeting spaces on the first floor and open plan office spaces on the 2nd–4th floors, which primarily house non-profit environmental activist organizations.

The design teams put together a design promoting low energy consumption. The goal of a low energy building was achieved through an integrated design process that combined thermal mass, shading, insulation, and daylighting strategies into an efficient building envelope, combined with efficient electric lighting design and control strategies, and a low energy HVAC system. The primary space conditioning subsystem is hydronic in-slab radiant cooling and heating, which is installed in the exposed ceiling slab of the 2nd–4th floors of the building. Due to their large surface area and high thermal mass, slab integrated radiant systems use relatively higher chilled water temperatures and lower hot water temperatures compared to traditional well-mixed air systems. In this building, the chiller is eliminated; the only cooling source is a cooling tower with a variable speed fan and the heating source is two condensing boilers that provide low temperature hot water at high efficiency. Besides radiant slab systems, the cooling tower and the condensing boilers also serve two dedicated outdoor air units that provide air at neutral temperature year-round to the spaces via an underfloor air distribution (UFAD) system. Natural ventilation is available through occupant controlled operable windows. The schematic diagram of the zone level HVAC system is presented in Fig. 1.

The building was LEED Platinum certified, and the 2012 utility data shows that the total building energy consumption was 37.9% lower than a prototype medium office building that complies with the 90.1-2007 standard. A web-based occupant satisfaction survey was conducted in 2010. Although the building was still undergoing commissioning work on the HVAC system at the time, the ratings from DBC are significantly higher when compared to a large benchmark database, containing 52,934 individual survey responses collected from over 475 buildings since 1997 [32].

4. EnergyPlus model

A single-story EnergyPlus (v8.0) model was developed based on the 3rd floor of the David Brower Center. Fig. 2 shows the floor plan and radiant slab thermal zones in the building, together with the thermostat locations. Zones core west and core east are combined into one single internal thermal zone for simplification in the EnergyPlus model. The south and north zone radiant systems are designed to cover only the area within 5 m of the exterior wall. As a result, it is possible that one physical office can be conditioned by two radiant systems at the same time. For those instances, an air wall with minimum resistance was simulated to separate the two radiant thermal zones.

4.1. Base model specifications

Data from construction documents and system schedules were used to develop the simulation model. Typical construction assemblies and thermal properties of materials used in the simulation are listed in Appendix A. The overall U factor for the exterior wall is 1.25 (W/m^2 K). The windows have a U factor of 2.425 (W/m^2 K) and SHGC at 0.39. Window to wall ratios are about 53% on the north, east and south sides. The building is well shaded by surrounding buildings/trees, exterior fixed overhangs and fins (South/East facade), and interior roller shades (North/South/East). Interior shades were simulated to be active when beam solar density on the windows exceeds 200 W/m^2.

The lighting and plug load usage profiles are developed based on sub-metered data from the year 2012 when the building was almost fully occupied. The density was obtained by averaging the hourly data for weekdays and weekends separately. The design plug load and lighting load densities were determined to be 5.42 W/m^2 and 2.54 W/m^2, respectively. Weekday and weekend schedules implemented in the EnergyPlus model are shown in Appendix A. Note that the lighting schedule for summer (April–October) and winter months are significantly different from each other. The measured peak lighting and equipment load densities were found only one third of the design values. Occupant density was obtained by counting workstations in each zone and Title 24 standardized schedule was implemented in the EnergyPlus model.

The radiant system was modeled based on the design document, and the details can be found in Appendix A. The water tubes were embedded 0.0508 m beneath the concrete surface, and the tube spacing was 0.15 m. A temperature sensor is embedded in each ceiling slab to monitor radiant surface temperature. Since only one typical floor was modeled, the HVAC equipment sizes at the plant level were scaled down based on floor area. These include the air-handling unit, pumps, boilers and cooling tower. The air-handling units were modeled to provide minimum ventilation air (0.00746 m^3/m^2) that feed into the space from the floor plenums. Air diffusers (42 in total) were uniformly distributed on the floor according to the design documents. Natural ventilation was also modeled, and 5% of the total window areas were modeled as operable (10% of the window area was operable, but field observation indicated at most 50% of them were in use by occupants).

4.2. Base model evaluation

4.2.1. Radiant system performance

To test EnergyPlus's capability in capturing radiant slab systems, a heating test was conducted during June 10–11th, 2011 (see Fig. 3). During this experiment, with monitored zone radiant loop valve manually opened, hot water at 32 °C flushed through the pipes for

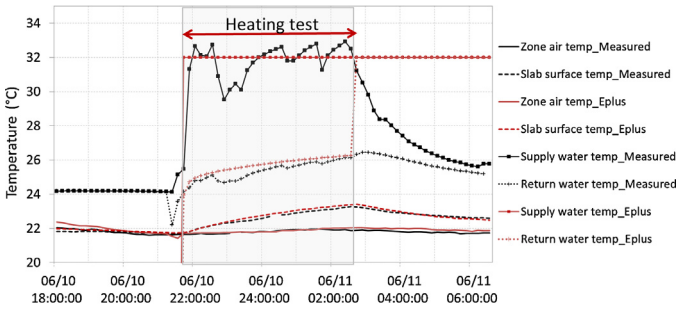

Fig. 3. Comparison of measured and predicted temperatures during heating pulse test.

4 h from 10:00 pm to 2:00 am when disturbances from internal load and ventilation system were at minimum level. The south perimeter zone on the 3rd floor was selected for this test and data loggers were installed to collect supply/return water temperatures, slab surface temperatures, and zone air and globe temperatures. It can be seen that EnergyPlus is able to capture the radiant system performance accurately during the testing period. Note that after the test was ended, simulated supply and return water temperature are not the same as the measured values. The measured temperatures here reflect the cool down process of the still water in the pipes after the water valve was closed, while EnergyPlus is not capable to capture this dynamic. There is an unrealistic jump in the simulated return water temperature. This is because in the world of simulation, when the water flow rate becomes zero, return water temperature is assumed to be the same as supply water temperature, which stays at its setpoint.

4.2.2. Monthly energy consumption

The simulation model was calibrated with measured 2012 heating and cooling energy usage as well as electrical energy usage for lighting and equipment. The operating stuff adjusted the systems in the first couple of years of operation. By 2012 the building was operating as intended with a high occupant satisfaction level in terms of thermal comfort, air quality, lighting, etc [32]. Due to the lack of a local weather station, Oakland TMY3 weather file was modified with locally measured outside dry bulb and wet bulb temperatures for simulation.

To evaluate how well the simulation model represents the measured data (Table 1) normalized mean bias error (NMBE) and coefficient of variation of the root mean squared error (CVRMSE) values were calculated using the following formulae [33]:

$$\mathrm{NMBE} = \frac{\sum_{i=1}^{n}(y_i - \breve{y}_i)}{(n-p)\times \bar{y}} \times 100 \qquad (1)$$

Table 2
Modeling uncertainties of the simulation model.

	ASHRAE Guideline 14[a] (%)	Internal load (%)	HVAC heating (%)	HVAC cooling (%)
NMBE	5	1.7	5.8	1.8
CVRMSE	15	4.39	13.81	7.6

[a] ASHRAE Guideline 14 (2002) whole building calibrated simulation path compliance requirements for monthly calibrated data.

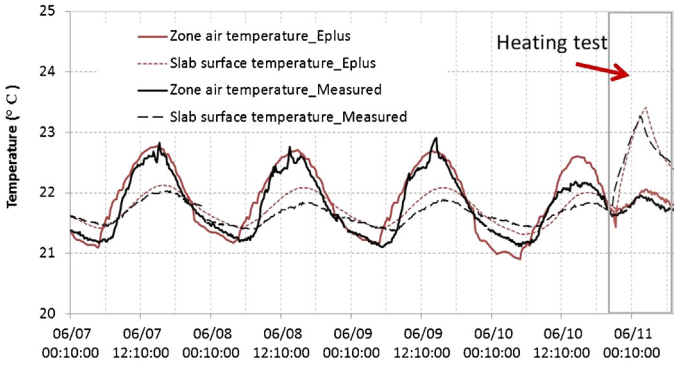

Fig. 4. Comparison of simulated and measured zone air temperature and slab temperature (South zone on 3rd floor).

$$\mathrm{CVRMSE} = \frac{\left[\sum_{i=1}^{n}(y_i - \breve{y}_i)^2/(n-p)\right]^{1/2}}{\bar{y}} \times 100\% \qquad (2)$$

For each evaluated category, as shown in Table 2, all simulated energy usage intensities, except HVAC heating, satisfy the ASHRAE Guideline 14 specified compliance, namely NMBE lower than 5% and CVRMSE lower than 15%. Note that the HVAC heating consumption NMBE value was 5.8%, which is only slightly higher than the 5% threshold. The error was acceptable given many other differences between the EnergyPlus model and the actual building, including: (1) the EnergyPlus model only consists of the third floor of the building; (2) real time solar data was not available for the simulation.

4.2.3. Thermal comfort

Detailed field measurements were conducted in the south zone for one week in June 2010. Fig. 4 compares the field measured and simulated air and slab surface temperatures. On June 10th, the simulated room temperatures are higher than measured temperatures, and this is due to the mismatch of the solar radiation data from the weather file and the reality. Note that in the last night, the room air temperature and radiant slab surface temperature increased due to the pulse-heating test mentioned in Section 4.2.1. Fig. 5 compares

Table 1
Comparison of measured and simulated monthly energy usage intensity.

Month	Internal load (kWh/m^2)		HVAC heating (kWh/m^2)		HVAC cooling (kWh/m^2)	
	Measured	Simulated	Measured	Simulated	Measured	Simulated
1	3.09	3.14	9.44	9.98	0.42	0.40
2	2.93	2.84	8.47	8.74	0.32	0.30
3	3.15	3.14	8.19	7.06	0.33	0.34
4	3.05	2.94	6.24	5.83	0.44	0.45
5	2.88	3.02	4.89	4.90	0.45	0.42
6	2.79	2.87	3.22	3.82	0.54	0.54
7	3.06	2.98	3.32	3.73	0.55	0.50
8	2.83	3.02	2.92	3.74	0.44	0.44
9	2.79	2.87	3.01	3.54	0.38	0.45
10	2.91	3.18	2.84	4.61	0.41	0.39
11	2.90	2.98	5.76	5.74	0.35	0.36
12	2.53	2.46	8.32	8.53	0.38	0.33

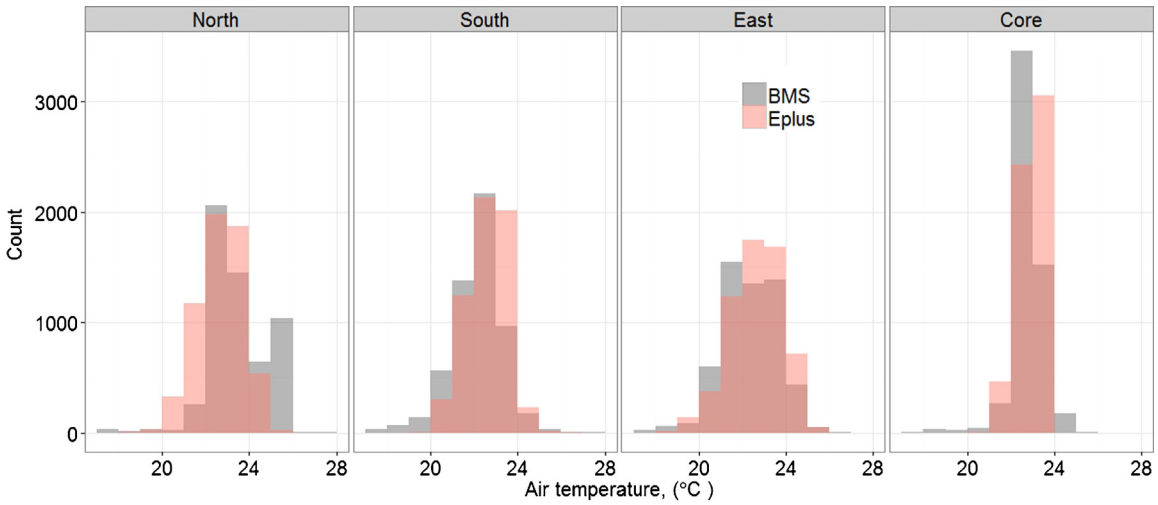

Fig. 5. Comparison of simulated and measured annual zone air temperatures using histograms (DBC 3rd floor).

the measured and simulated air temperatures for all zones (year 2012) in the building using histograms. The measured data was obtained from the building management system. Both figures indicate that the EnergyPlus model does a good job of capturing the thermal comfort environment in the building.

5. Control methods

There are in total four thermal zones, and each is individually conditioned by a radiant slab loop with a control valve. While slab heat is available year-around, slab cooling in the summer season can be limited with the cooling tower as the only cooling source. The lowest water temperature a cooling tower can theoretically produce is the outdoor air wet bulb temperature. However, an approaching temperature of within 3–5 °C of the outdoor wet bulb temperature is usually what can be achieved in practice. Consequently, for the hot and humid days when cooling demand is the highest, cooling capacity is limited. This imposes a practical limitation on cold water temperature. On the other hand, because the cold water is generated by a cooling tower, the risk of condensation can be minimized and thus omitted when developing the control algorithm. Besides the radiant slabs, additional cooling may be available through natural ventilation from occupant controlled operable windows. Cooling capacity from the mechanical ventilation system during occupied hours is however limited because only neutral air will be supplied. In fact, even neutral air may not be guaranteed during the periods with high outside air temperature. Considering the complexity of the problem in the cooling application, we focused our attention to summer operation. One key decision to make about the slab control strategy is how to precharge the radiant slabs so that there is enough cool energy storage for maintaining comfort throughout a day without overcooling the space in early morning. Condensing water temperature setpoint was set to 15.5 °C when cooling tower was called. Note the actual water temperature may not reach this setpoint depending on the outside wetbulb temperature.

5.1. Heuristic rule based control

Heuristic control algorithms implemented in the DBC building were modified and implemented in EnergyPlus:

(1) There is a modulating valve on each loop that was controlled to maintain a zone heating or cooling set point. While heating is available year-around, slab cooling is available through pre-conditioning during unoccupied hours (between 10:00 pm and 6:00 am). Cooling during occupied hours is limited with room cooling setpoint at 25 °C with a 2 °C throttling range, i.e. the water flow valve starts to open when the room temperature rises to 24 °C and reaches 100% when the temperature is 26 °C. Fig. 6 plots the radiant system heating and cooling setpoint for both occupied and unoccupied hours for the summer season;
(2) Precooling is only activated if the highest outdoor air temperature of the previous day has exceed 28 °C;
(3) If precooling is not activated, the room cooling setpoint is 24 °C and heating setpoint is 18 °C for the entire day;
(4) During cooling periods, when radiant water supply temperature is less than 1 °C lower than room operative temperature, the water flow valve is shut off;
(5) When precooling is activated, nighttime ventilation is also turned on to maintain the same precooling setpoint at 20 °C.

Compared to the current control sequence in the DBC, the tested control is different, including: (1) instead of an on/off control, the valves were simulated to be able to modulate between 0 and 100%; (2) in existing control, cooling is not available during occupied hours. For the test, cooling will be provided if room temperature exceeds a threshold. These changes were made because they were able to improve thermal comfort conditions compared to the existing control sequences.

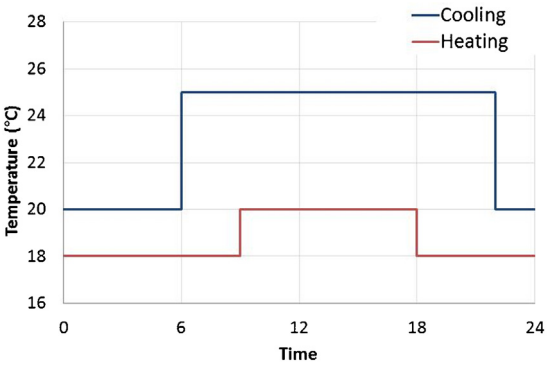

Fig. 6. Radiant slab system heating and cooling set point schedule (precooling is activated only when maximum outdoor air temperature of the previous day exceeds 28 °C).

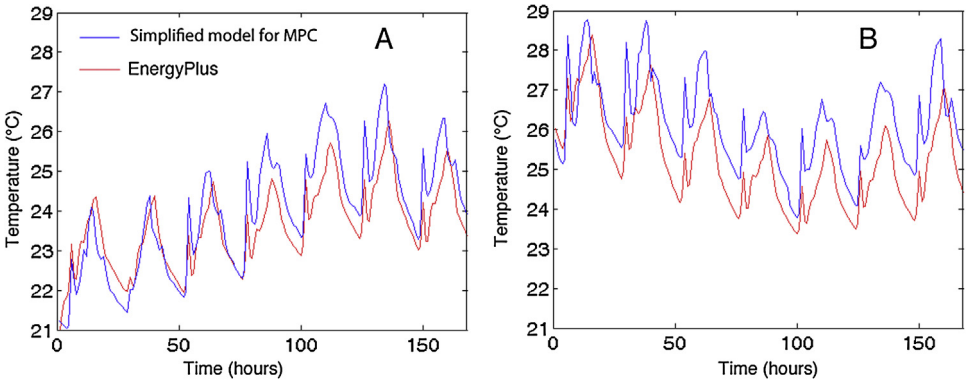

Fig. 7. East zone MPC model open-loop validation: (A) cooling mode; and (B) coasting mode.

5.2. Model predictive control

5.2.1. Model development

A good review of existing modeling method for radiant system can be found in [34]. The goal here is to create a simplified dynamic model of a radiant slab system for use in the MPC The model should predict room temperatures within tolerable bounds over some specified horizon. We propose a second-order model with the following two states: room air temperature, T_a, and the temperature of the slab, T_s, Other masses in the room, such as walls, are assumed to have temperatures close to the room air temperature [35]. We also assume that there are no thermal interactions between the adjacent rooms.

Using basic energy balance concepts, we can derive the following state equation for zone air temperature:

$$m_a C_p \frac{dT_a}{dt} = C_p \dot{m}_{a_{in}}(T_{a_{in}} - T_a) + P_{dis} + (1-\beta)P_{int} + (1-\alpha)G_s - U_{rs}A_{rs}(T_a - T_s) - \sum_{i=0}^{N} U_{ra,i}A_{ra,i}(T_a - T_{z,i}) - U_{ro}A_{ro}(T_a - T_o) \quad (3)$$

Note that the heat transfer coefficients need not be constants. Karadag [36] suggested using $U_{rs} = k|T_a - T_s|^{0.09}$.

To obtain the state equation for slab temperature, we model the convective heat exchange between the slab and water in the pipes as follows assuming the slab temperature is uniform [37]:

$$q_w = U_w \pi DL \Delta T_{lm} \quad (4)$$

where

$$\Delta T_{lm} = \frac{\Delta T_o - \Delta T_i}{\ln(\Delta T_o / \Delta T_i)}$$
$$\Delta T_o = T_s - T_{w_o}$$
$$\Delta T_i = T_s - T_{w_i}$$
$$\frac{\Delta T_o}{\Delta T_i} = \exp\left(-\frac{\pi DL}{\dot{m}_{w_{in}} C_{p,w}} U_w\right)$$

Then, we can derive the following state equation for slab temperature:

$$m_s C_{p,s} \frac{d}{dt} T_s = UA(T_a - T_s) + \alpha G_s + \beta P_{int} - U_w \pi DL \Delta T_{lm} \quad (5)$$

5.2.2. Model linearization and discretization

In the David Brower Center, the water valves provide binary input to the radiant slabs. Either the water valve is full on or full off. Therefore, we propose to use a switched discrete linear model to represent our system. Let $T_t = [\, T_{a,t} \quad T_{s,t} \,]^T$ be the state vector and let h_t and c_t be the indicator variable for the hot and cold water valve positions, respectively. Then,

$$T_{t+1} = \begin{cases} A_{\text{cool}} T_t + w_t \text{ if } c_t = 1, h_t = 0 \\ A_{\text{heat}} T_t + w_t \text{ if } c_t = 0, h_t = 1 \\ A_{\text{coast}} T_t + w_t \text{ if } c_t = 0, h_t = 0 \end{cases} \quad (6)$$

Note that the cooling models were averaged over a range of supply water temperatures. This simplification can reduce model complexity and was tested as valid, because the responses of the slab and the space were slow to changes in water temperature between 15 and 20 °C. In cooling tests, we set the cold water supply temperature to the outdoor wetbulb temperature plus 3 °C. This was found in preliminary tests to be close to optimal. The heating water temperature was set as a constant at 32 °C. Here, w_t is the average net effect of external disturbances to the system, which includes solar loads, internal loads, and outside air temperature. The use of average disturbance is discussed in Section 5.2.5.

5.2.3. Model validation

In order to validate the correctness of the model, we have identified the model parameters for the calibrated EnergyPlus model of DBC by performing step test simulations. Then, we run the model against a different data set to verify the correctness of the model.

Fig. 7 shows a weeklong open-loop validation of the linear cooling and coasting model for the east zone of the Brower Center. The coasting model for this particular zone had a maximum temperature error of 0.968 °C and an average temperature error of 0.3043 °C over the weeklong period. The cooling model for this particular zone had a maximum temperature error of 1.1239 °C and an average temperature error of 0.8493 °C over the weeklong period.

5.2.4. Problem formulation

The goal of MPC is to choose the water valve position so that a weighted combination of comfort violation and energy usage is minimized over a prediction horizon N. The controls decision is formulated as an optimization problem with constraints.

Let $T_{\max,t}$ and $T_{\min,t}$ be the maximum and minimum desired air temperatures at time t, respectively. The finite-horizon optimization problem we are solving is

$$\min_{\{c_k, h_k\}} \sum_{k=t}^{t+N} \rho \max\{T_{a,k} - T_{\max,t}, T_{\min,t} - T_{a,k}, 0\} + (c_k + h_k)$$

Subject to

$$T_{t+1} = \begin{cases} A_{\text{cool}} T_t + w_t \text{ if } c_t = 1, h_t = 0 \\ A_{\text{heat}} T_t + w_t \text{ if } c_t = 0, h_t = 1 \\ A_{\text{coast}} T_t + w_t \text{ if } c_t = 0, h_t = 0 \end{cases}$$

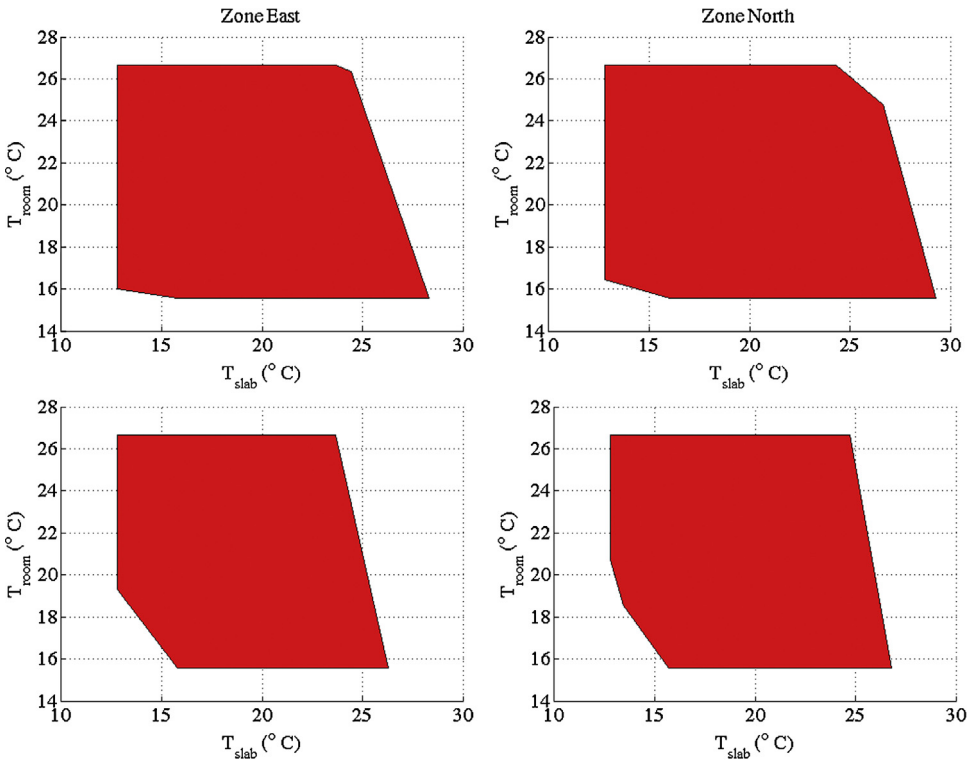

Fig. 8. Set of initial values of T_t for which certainty equivalence is exact.

where, ρ is a weight to adjust between energy savings and comfort satisfaction. In our experimental runs, $\rho = 1000$, $T_{max} = 26\,^{\circ}C$ and $T_{min} = 22\,^{\circ}C$.

5.2.5. Stochastic disturbances

External disturbances, w_t, are in reality uncertain and hard to predict. In controls problems they are often modeled as random variables. The usual approach is to minimize the expected cost, which is now also a random variable. However, the exact feedback solution to this problem is generally intractable. There are several approximate approaches available, among them the simplest of which is to replace w_t with its expected value. This technique is known as certainty equivalence. While an attractive solution because of its simplicity, it is potentially a bad estimate of the original problem. However, certainty equivalence applies well to the radiant slab problem.

For a similar optimization problem as above, the set of states for which certainty equivalence can be applied can be explicitly computed [32]. Fig. 8 shows the set of room and slab temperatures for which certainty equivalence can be applied for our radiant slab system. See Appendix B for the calculation process. Note that the computed region covers almost the entire operating regime. This shows that for the system and problem under consideration, there is little value in knowing the distribution of the disturbance.

5.2.6. Implementation

The problem as formulated above is a mixed-integer program. While the problem is in general difficult to solve (there is a combinatorial explosion in computation time), there are efficient solvers available to solve most problems in reasonable time. We used IBM ILOG CPLEX to solve the mixed-integer program in Matlab. In order to interface in closed-loop with the EnergyPlus model of DBC, we use MLE+ [38]. MLE+ is a Matlab-based toolbox for EnergyPlus/Matlab co-simulation.

6. Comparison of control methods

For assessment of the effectiveness of control methods we chose not to run the tests using the weather file of the building site because the mild climatic conditions of the sites provides limited opportunity for the radiant cooling system to operate at all. Instead, Sacramento, CA, representing more severe climate conditions, was selected for the tests. Simulation results from a summer season (June–August) were analyzed here.

6.1. Thermal comfort

Thermal comfort can be assessed through thermal comfort categories introduced by the EN 15251 [39] standard. This method of representing the results describes the percentage of occupied hours when the operative temperature exceeds the specified range. During summer operation, for clothing level at 0.55, air speed at 0.12 m/s, metabolic rate at 1.2 and humidity level at 50%, the operative temperature range to achieve Category II (Predicted Percentage Dissatisfied (PPD) < 10%) is 23–26 °C and for Category III (PPD < 15%) the range is 22–27 °C. For long term performance, according to EN 15251 [39] Appendix G, the recommended criteria for acceptable deviation is that the percentage of exceedance be less than 5% of occupied hours of a day, week, month, and year.

Fig. 9 compares the thermal comfort level for each zone using MPC and heuristic methods. For simplification, the percentages are labeled only for Categories II and III. Overall, the MPC controller was able to maintain zone operative temperatures at Category II thermal comfort level more than 95% of the occupied hours for all zones. With the heuristic method, only the core zone operative temperatures were maintained at Category II level for more than 95% of the occupied hours; for the east zone, only 88.3% of the time. In addition, the MPC controlled zones reached Category IV only 1.3% of the time (the highest zone operative temperature was 27.6 °C and the minimum was 20.6 °C, and both incidents were happened in the

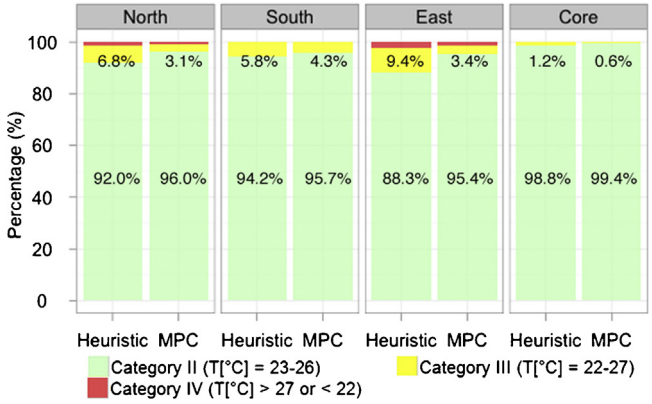

Fig. 9. Comparison of thermal comfort performance of MPC and heuristic control method based on EN 15251 Catogories for a typical summer season in Sacramento, CA (June–August).

west zone), while the heuristic method controlled zones reached Category IV 2.5% of the time (the highest zone operative temperature was 27.5 °C in the west zone and the minimum was 21.7 °C in the core zone).

6.2. Energy consumption

The itemized HVAC energy consumptions are presented in Fig. 10 Compared to the heuristic control method, MPC reduced total energy consumption by 14.4%. For cooling tower energy consumption, it is a 55% reduction, and for pumps, it is 26%.

6.3. Examples of MPC and heuristic control from the test

To obtain some granularity of the controller performance, Figs. 11 and 12 present zone operative temperatures and valve operating conditions for two example days from the test.

The first example (Fig. 11) shows the east zone conditions on July 09th, which features a range of outdoor air temperature from 18.3 °C at 4:00 am to 39.0 °C at 6:00 pm. The wetbulb temperature ranges from 14 to 20 °C, and the cooling tower was able to generate cold water at temperatures from 19 to 25 °C. With the morning sun hitting the window and later triggering the interior blinds to come down, there was a bump in zone operative temperature in the morning. With the heuristic control, as the maximum outdoor air temperature of the previous day exceeded 28 °C, precooling was kicked on from 10:00 pm on the previous day to 6:00 am. The system then stayed off until about 10:00 am when zone operative temperature rose to 24 °C. At 3:00 pm, outdoor wetbulb temperature is too high and the cooling tower was no longer able to generate

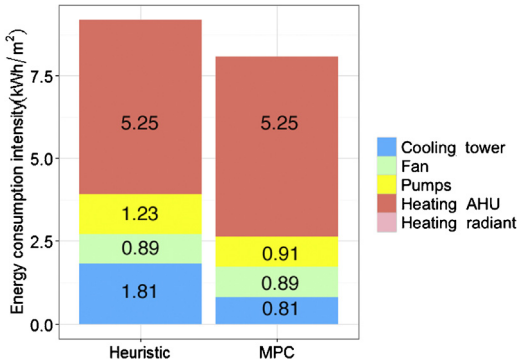

Fig. 10. Comparison of energy consumptions between MPC and heuristic methods (June–August).

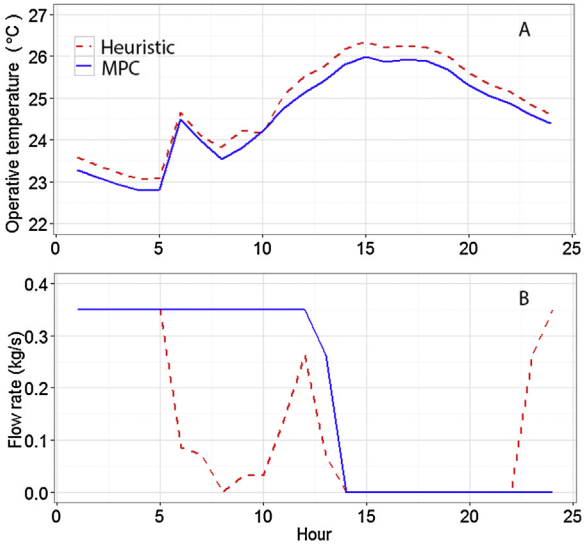

Fig. 11. Comparison of Heuristic and MPC methods in control of zone operative temperature (A) and radiant loop valve (B): East zone on July-09th.

water with temperature cool enough and the valve shut off. Zone operative temperature swung from around 23 °C early in the morning to a peak of 26.5 °C at 3:00 pm. While with the MPC controller, with the predictive knowledge of high cooling demand throughout the day, radiant cooling continues until 3:00 pm and zone operative temperature was maintained well below 26 °C, which was set as the upper boundary for thermal comfort in the controller.

The second example (Fig. 11) shows the south zone conditions on July 26th, which features a range of outdoor air temperature from 13.0 °C at 3:00 am to 34.0 °C at 5:00 pm. The wetbulb temperature ranges from 12.5 to 20.1 °C, and the cooling tower was able to generate cold water at temperatures from 18.9 to 24.7 °C. With the heuristic control, precooling was kicked on until 6:00 am according to the rule. Zone operative temperature swung from around 22.5 °C early in the morning to a peak of 25.1 °C at 5:00 pm. While with the MPC controller, cooling was considered not necessary for the whole day and zone operative temperature was maintained within a 23–25 °C range throughout the day.

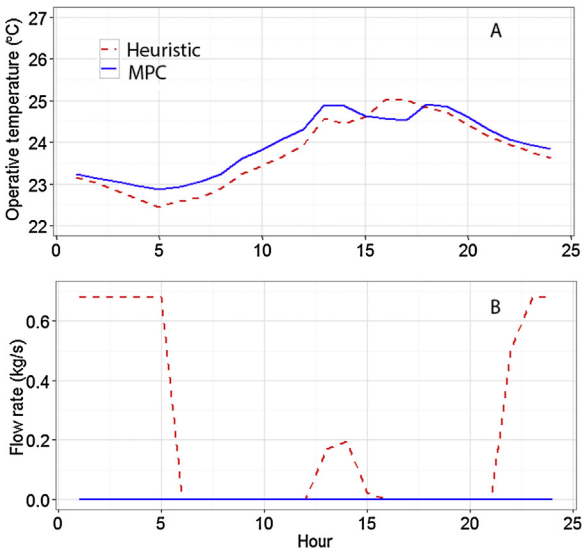

Fig. 12. Comparison of Heuristic and MPC methods in control of zone operative temperature (A) and radiant loop valve (B): South zone on July-26th.

Based on these two examples, MPC, with the capability to use predictions of the cooling demand and the thermal response of individual zones, was able to make wise decision on when to turn on/off zone level radiant systems to conserve energy and maintain thermal comfort.

7. Conclusions

In this paper, we studied the control of the heavyweight radiant slab system for a typical office building. In this building, the chiller is eliminated and the only cooling source is a cooling tower. This means the system has limited cooling capability when outdoor wetbulb temperature is high. Model predictive control (MPC) was tested against a fine-tuned rule based heuristic control method for this complex control problem. A first-order dynamical model was developed for implementation in the model predictive controller and it was shown to be able to predict system performance reasonably well.

The test was conducted for a summer season in a dry and hot climate and the MPC controller using the first-order system model was able to maintain zone operative temperatures at EN 15251 Category II thermal comfort level more than 95% of the occupied hours for all zones. With the heuristic method, only the core zone operative temperatures were maintained at Category II level for more than 95% of the occupied hour; for the east zone, the number was only 88.3%. Compared to the heuristic method, MPC reduced the cooling tower energy consumption by 55% and pumping power consumption by 25%.

Acknowledgments

This work was supported by the California Energy Commission (CEC) Public Interest Energy Research (PIER) Buildings Program (CEC 500-08-004). Partial funding was also provided by the Center for the Built Environment, University of California, Berkeley (www.cbe.berkeley.edu). We would like to express our appreciation to the staff at the David Brower Center for assisting with field measurements. We would also like to thank the engineers from Integral Group for providing design information of the building.

Appendix A. Building-modeling information

Construction and geometry

The overall U factor for the exterior wall is 1.25 (W/m^2 K). Windows have a U factor of 2.425 (W/m^2 K) and SHGC at 0.39 (Table A1–A2).

Shading system

The building is well shaded by surrounding buildings/trees, exterior fixed overhangs and fins (South and East facade), and interior roller shades (North/South/East). See Fig. A1. Both interior shade, exterior shade and the surrounding buildings were modeled in EnergyPlus.

Table A2
Window-wall Ratio in EnergyPlus.

Total	North	East	South	West
Window-Wall ratio (%)	53.59	53.4	45.62	6

Table A3
EnergyPlus radiant system modeling information.

Radiant zones	Total flow rate (m^3/s)	Total loop length (m)	Tube diameter (m)
South	0.000687	809	
North	0.00065	809	
East	0.00028	516	0.0159
West	0.00024	435	
Core	0.00035	675	

Internal load

The lighting and plug load usage data are obtained from submetered data. The internal load density was obtained by averaging the hourly measured data for weekdays and weekends separately. Weekday and weekend schedules used in the EnergyPlus model are shown in Fig. A2.

HVAC system information

Schematic of the complete hydronic system is in Fig. A3. Cold water supplied from the cooling tower serves, via a heat exchanger, the cooling coils in the two dedicated fresh air units, and the radiant loops. The cooling tower modeled has a total capacity of 53 kW, a design air flow rate at 4.25 m^3/s, and the design fan power was at 2 kW. Hot water provided by two condensing boilers serves the two fresh air units, and the radiant loop. The simulated HVAC system is developed based on the DBC design, but scaled proportionally based on floor area for serving only the third floor and the system was simplified for modeling purposes. One example of such simplification is that only one air-handling unit was modeled to provide ventilation air.

The supply air temperatures from the ventilation units was reset from18 to 22 °C when outdoor air temperature changes from 21 to 15 °C.

Radiant system

Radiant slab systems' modeling specifications are summarized below. These were developed based on original design documents (Table A3).

Appendix B. Computing system states satisfying certainty equivalence

Consider the following radiant-slab system implemented at the Brower Center in Berkeley, CA. The system can be represented by the state vector $T_t = [\, T_{a,t} \quad T_{s,t} \,]^T$, where $T_{s,t}$ is the temperature of the radiant slab and $T_{a,t}$ is the temperature of the room. Let u_t be the temperature of the water supplied to the radiant slab, and d_t is

Table A1
Construction specifications.

External wall	Internal wall	Ceiling	Window
Gypsum board	Gypsum board		U factor: 2.43 W/m^2-K
2 1/2″ Insulations	2 1/2″ Air gap		
5/8′ Densglass sheathing			SHGC: 0.39
Ribbed Metal Siding	Gypsum board	6″ heavy weight concrete	

Fig. A1. DBC interior roller shade (left) and exterior fixed shades (right) on south façade.

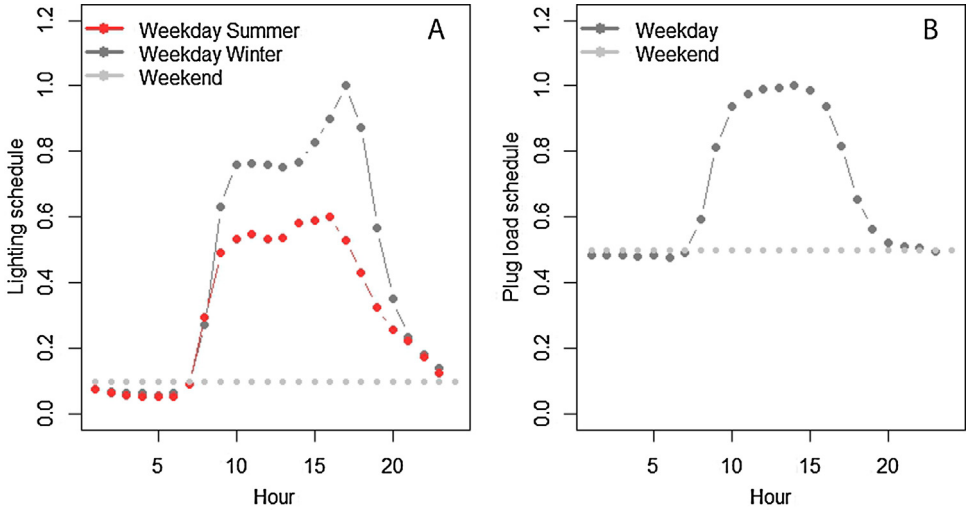

Fig. A2. Internal load schedule used in EnergyPlus model: (A) lighting; (B) Plug load.

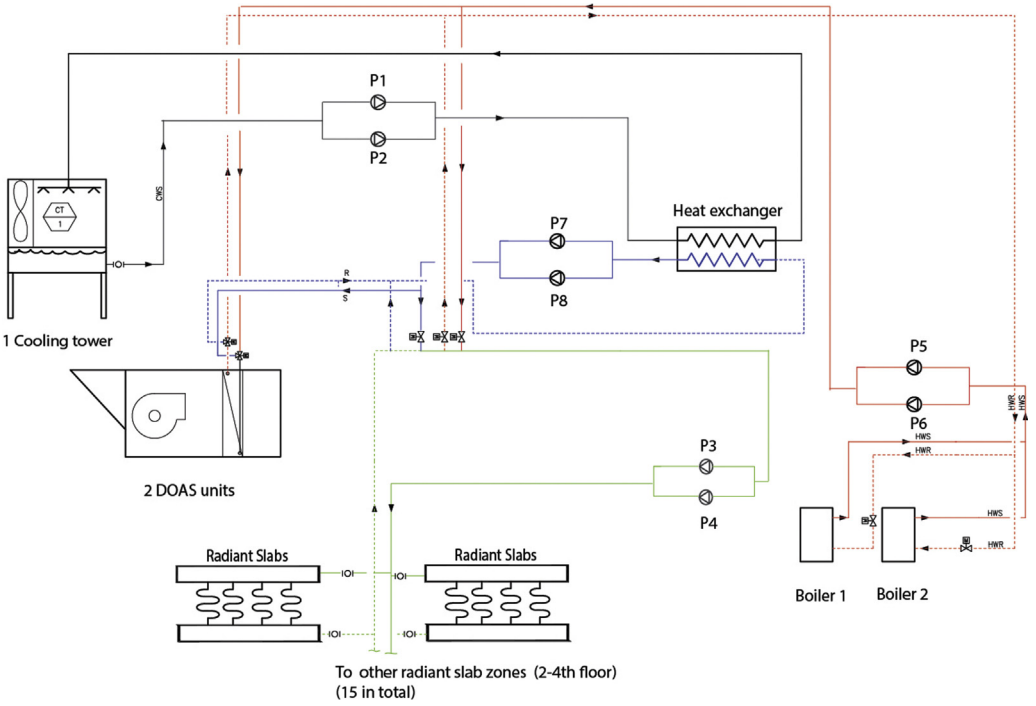

Fig. A3. Schematics of the hydronic loop.

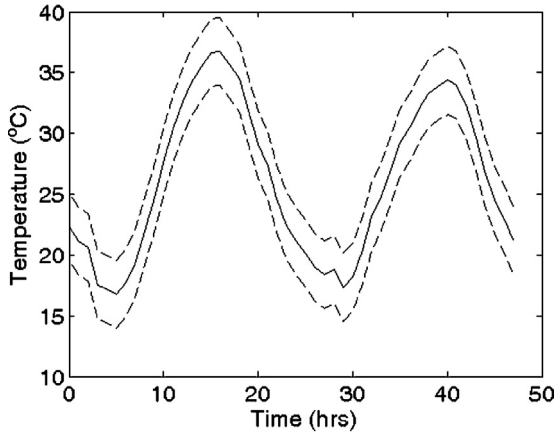

Fig. B1. Outside air temperature.

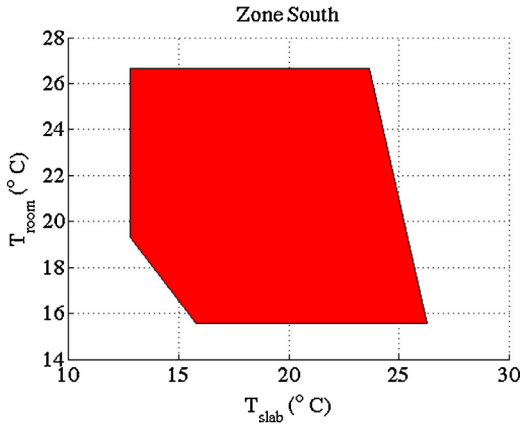

Fig. B2. Set of initial values of T_t for which certainty equivalence is exact.

the outside air temperature at time t, with time measured in hours The radiant slab system can be approximated by a linear system update equation of the form

$$T_{t+1} = AT_t + Bu_t + Wd_t$$

where A, B, W are parameters can be identified by performing step-tests on the actual building.

We are interested in controlling the water temperature supplied to the slabs to maintain the room air temperature close to a comfortable temperature of 22 °C. The supply water temperature is constrained to be within 12.7 °C and 32 °C. We investigated controlling the building temperature on a hot summer day, with a 48 h outside air temperature prediction, OAT_t, as shown in Fig. B1.

Assume that the weather prediction has a 2.5° radius uncertainty, which is shown by the dotted bounding lines above and below the nominal temperature profile. Suppose that we wish to maintain the room temperature, $T_{a,t}$, close to an optimal temperature of 22 °C while minimizing energy usage. Suppose that the water supply temperature, u_t, has a nominal temperature of 22 °C and that changing the water temperature from the nominal temperature will require energy. Suppose for a horizon of N hours we would like to minimize the cost:

$$E\left(\sum_{t=0}^{N-1}[(T_{a,t}-22)^2+\rho(u_t-22)^2]+(T_{a,N}-22)^2\right)$$

subject to the robust constraint $\begin{bmatrix}12.7\\15\end{bmatrix} < T_t < \begin{bmatrix}32\\26\end{bmatrix}$. In order to write the cost as a quadratic cost, we introduce new states $\bar{T}_t = T_t - \begin{bmatrix}0\\22\end{bmatrix}$, and $\bar{u}_t = u_t - 22$. By straightforward substitution, the state update equation becomes

$$T_{t+1} = A\bar{T}_t + B\bar{u}_t + A\begin{bmatrix}0\\22\end{bmatrix} + 22B - \begin{bmatrix}0\\22\end{bmatrix} + Wd_t$$

And the cost becomes

$$f_t(\bar{T}_t, \bar{u}_t) = \bar{T}_t^T \begin{bmatrix}0 & 0\\0 & 1\end{bmatrix} \bar{T}_t + \rho\bar{u}_t^2,$$

$$f_t(\bar{T}_N) = \bar{T}_N^T \begin{bmatrix}0 & 0\\0 & 1\end{bmatrix} \bar{T}_N$$

For a horizon of 6 h, Fig. B2 shows the set of initial states T_0 such that the certainty equivalence approximation can be used to obtain an exact solution to the original expected value problem.

The plot shows that for our radiant-slab system, the set of states for which certainty equivalence can be applied covers almost the entire operating regime. This shows that for the system and problem under consideration, there is little value in knowing the distribution of the disturbance.

References

[1] G.P. Henze, C. Felsmann, D.E. Kalz, S. Herkel, Primary energy and comfort performance of ventilation assisted thermo-active building systems in continental climates, Energy Build. 40 (2) (2008) 99–111.
[2] Z. Tian, J.A. Love, Energy performance optimization of radiant slab cooling using building simulation and field measurements, Energy Build. 41 (3) (2009) 320–330.
[3] J. Babiak, B. Olesen, D. Petras, REHVA Guidbook No. 7: Low Temperature Heating and High Temperature Cooling, 2nd ed., Federation of European Heating and Air-Conditioning Associations, Brussels, Belgium, 2007.
[4] J. Feng, S. Schiavon, F. Bauman, Cooling load differences between radiant and air systems, Energy Build. 65 (2013) 310–321.
[5] J. Feng, F. Bauman, S. Schiavon, Experimental comparison of zone cooling load between radiant and air systems, Energy Build. 84 (2014) 152–159.
[6] B. Olesen, Radiant floor cooling systems, ASHRAE J. 50 (9) (2008) 16–22.
[7] A. Odyjas, A. Gorka, Simulations of floor cooling system capacity, Appl. Therm. Eng. 51 (2013) 84–90.
[8] ISO, ISO-11855: 2012, Building Environment Design—Design, Dimensioning, Installation and Control of Embedded Radiant Heating and Cooling Systems, International Organization for Standardization, 2012.
[9] D.O. Rijksen, C.J. Wisse, A.W.M. van Schijndel, Reducing peak requirements for cooling by using thermally activated building systems, Energy Build. 42 (3) (2010) 298–304.
[10] J.E. Braun, Reducing energy costs and peak electrical demand through optimal control of building thermal storage, ASHRAE Trans. 96 (2) (1990) 876–888.
[11] G.P. Henze, T.H. Le, A.R. Florita, C. Felsmann, Sensitivity analysis of optimal building thermal mass control, J. Sol. Energy Eng. 129 (4) (2007) 473–485.
[12] D. Nikovski, J. Xu, M. Nonaka, A method for computing optimal set-point schedules for HVAC systems, in: Proceedings of the 11th REHVA World Congress-CLIMA, Czech Republic, Prague, 2013, p. 2013.
[13] B. Olesen, Possibilities and limitations of radiant cooling, ASHRAE Trans. 103 (1) (1997) 7.
[14] B. Olesen, Radiant floor heating in theory and practice, ASHRAE J. 43 (7) (2001) 19–24.
[15] K.A. Antonopoulos, M. Vrachopoulos, C. Tzivanidis, Experimental and theoretical studies of space cooling using ceiling-embedded piping, Appl. Therm. Eng. 17 (4) (1997) 351–367.
[16] P. Weitzmann, Modelling Building Integrated Heating and Cooling Systems, Department of Civil Engineering, Danmark Technisk Universite, 2004.
[17] M. Gwerder, B. Lehmann, J. Tödtli, V. Dorer, F. Renggli, Control of thermally-activated building systems (TABS), Appl. Energy 85 (7) (2008) 565–581.
[18] M. Gwerder, J. Todtli, B. Lehmann, V. Dorer, W. Guntensperger, F. Renggli, Control of thermally activated building systems (TABS) in intermittent operation with pulse width modulation, Appl. Energy 86 (9) (2009) 1606–1616.
[19] B. Lehmann, V. Dorer, M. Gwerder, F. Renggli, J. Todtli, Thermally activated building systems (TABS): energy efficiency as a function of control strategy, hydronic circuit topology and (cold) generation system, Appl. Energy 88 (1) (2011) 180–191.

[20] J. Hu, P. Karava, Model predictive control strategies for buildings with mixed-mode cooling, Build. Environ. 71 (2014) 233–244.
[21] Y. Ma, A. Kelman, A. Daly, F. Borrelli, Predictive control for energy efficient buildings with thermal storage: modeling, stimulation, and experiments, IEEE Control Syst. 32 (1) (2012) 44–64.
[22] F. Oldewurtel, A. Parisio, C.N. Jones, D. Gyalistras, M. Gwerder, V. Stauch, B. Lehmann, M. Morari, Use of model predictive control and weather forecasts for energy efficient building climate control, Energy Build. 45 (2012) 15–27.
[23] N.T. Gayeski, Predictive Pre-cooling Control for Low Lift Radiant Cooling using Building Thermal Mass, Department of Architecture, Massachusettes Institute of Technology, 2010.
[24] P.R. Armstrong, S.B. Leeb, L.K. Norford, Control with building mass-Part I: Thermal response model, ASHRAE Trans. 112 (1) (2006) 449.
[25] C.D. Corbin, G.P. Henze, P. May-Ostendorp, A model predictive control optimization environment for real-time commercial building application, J. Build. Perform. Simul. 6 (3) (2013) 1–16.
[26] B. Coffey, Using Building Simulation and Optimization to Calculate Lookup Tables for Control, Building Science in Architecture Department, University of California at Berkeley, 2011.
[27] P.T. May-Ostendorp, G.P. Henze, B. Rajagopalan, D. Kalz, Experimental investigation of model predictive control-based rules for a radiantly cooled office, HVAC&R Res. 19 (5) (2013) 602–615.
[28] D.B. Crawley, J.W. Hand, M. Kummert, B.T. Griffith, Contrasting the capabilities of building energy performance simulation programs, Build. Environ. 43 (4) (2008) 661–673.
[29] X. Pang, M. Wetter, P. Bhattacharya, P. Haves, A framework for simulation-based real-time whole building performance assessment, Build. Environ. 54 (2012) 100–108.
[30] R.H. Henninger, M.J. Witte, D.B. Crawley, Analytical and comparative testing of EnergyPlus using IEA HVAC BESTEST E100'ÄìE200 test suite, Energy Build. 36 (8) (2004) 855–863.
[31] V. Ghatti, Experimental validation of the EnergyPlus low-temperature radiant simulation, Transactions 109 (2) (2003) 614–623.
[32] F. Bauman, T. Webster, D. Dickerhoff, S. Schiavon, J. Feng, C. Basu, Case study report: David Brower Center, in: Internal Report, Center for the Built Environment, University of California, Berkeley, 2011.
[33] ASHRAE, ASHRAE Guideline 14-2002: Measurement of Energy and Demand Savings, in, American Society of Heating, Refrigerating and Air Conditioning Engineers Inc., Altanta, GA, 2002.
[34] X. Xu, S. Wang, J. Wang, F. Xiao, Active pipe-embedded structures in buildings for utilizing low-grade energy sources: a review, Energy Build. 42 (10) (2010) 1567–1581.
[35] C.L. Conroy, S.A. Mumma, Ceiling radiant cooling panels as a viable distributed parallel sensible cooling technology integrated with dedicated outdoor air systems, ASHRAE Trans. 107 (1) (2001) 578–588.
[36] R. Karadag, New approach relevant to total heat transfer coefficient including the effect of radiation and convection at the ceiling in a cooled ceiling room, Appl. Therm. Eng. 29 (8) (2009) 1561–1565.
[37] F.P. Incropera, A.S. Lavine, D.P. DeWitt, Fundamentals of Heat and Mass Transfer, John Wiley & Sons Incorporated, New York, USA, 2011.
[38] W. Bernal, M. Behl, T.X. Nghiem, R. Mangharam, MLE+: a tool for integrated design and deployment of energy efficient building controls, in: Proceedings of the Fourth ACM Workshop on Embedded Sensing Systems for Energy-Efficiency in Buildings, ACM, 2012, pp. 123–130.
[39] Cen, EN 15251-2007, Criteria for the Indoor Environment Including Thermal, Indoor Air Quality, Light and Noise, in, Brussels, 2007.